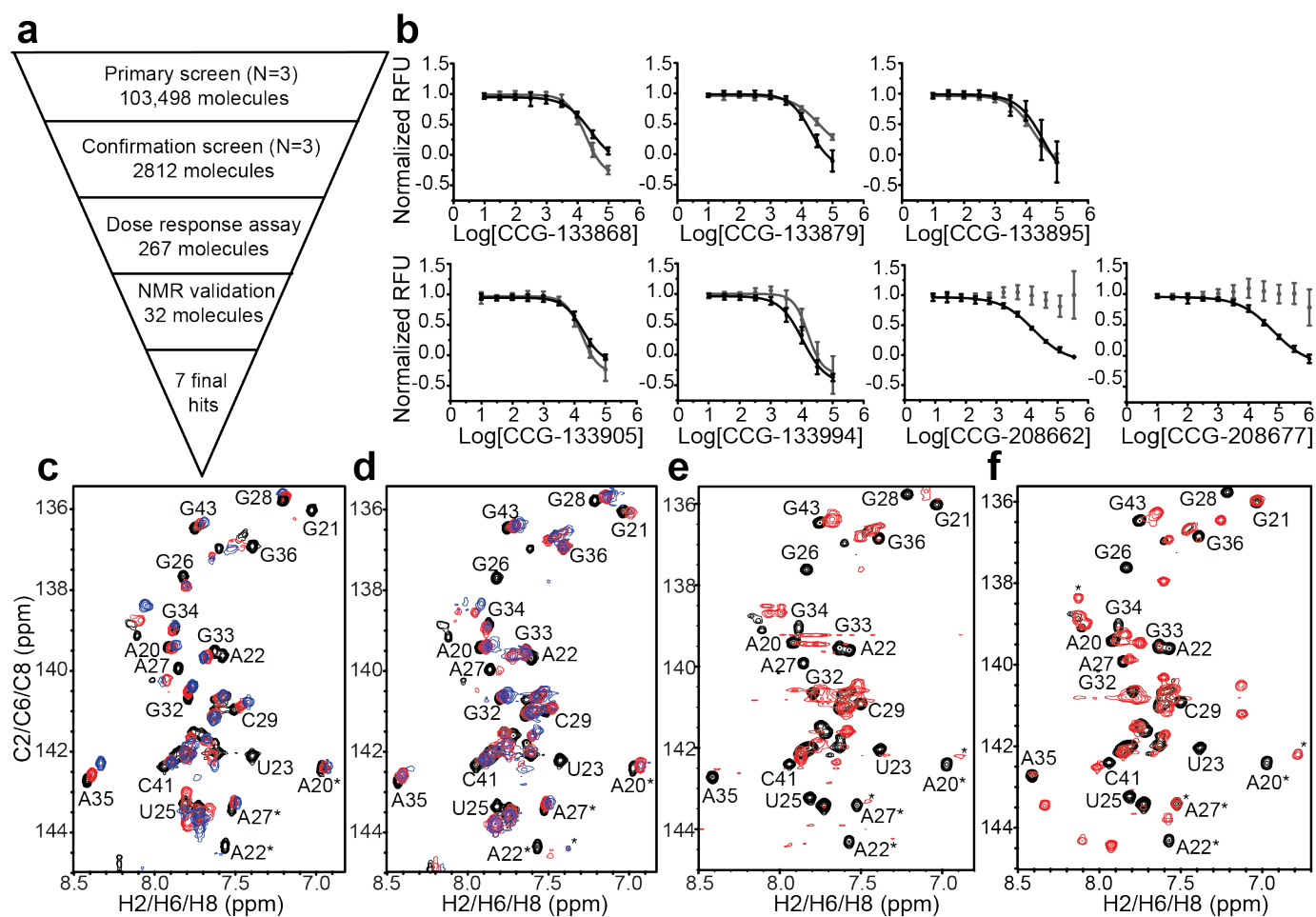
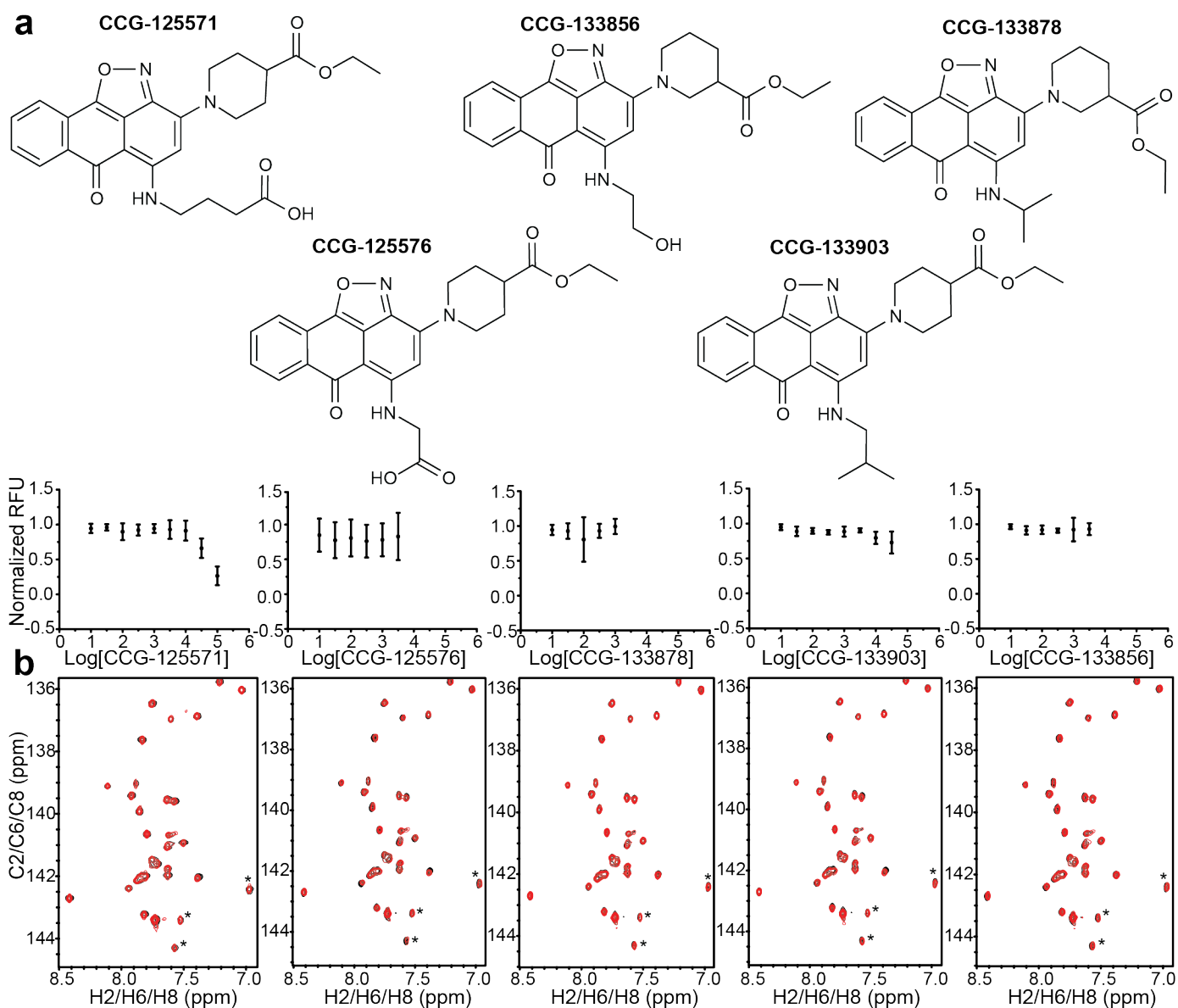


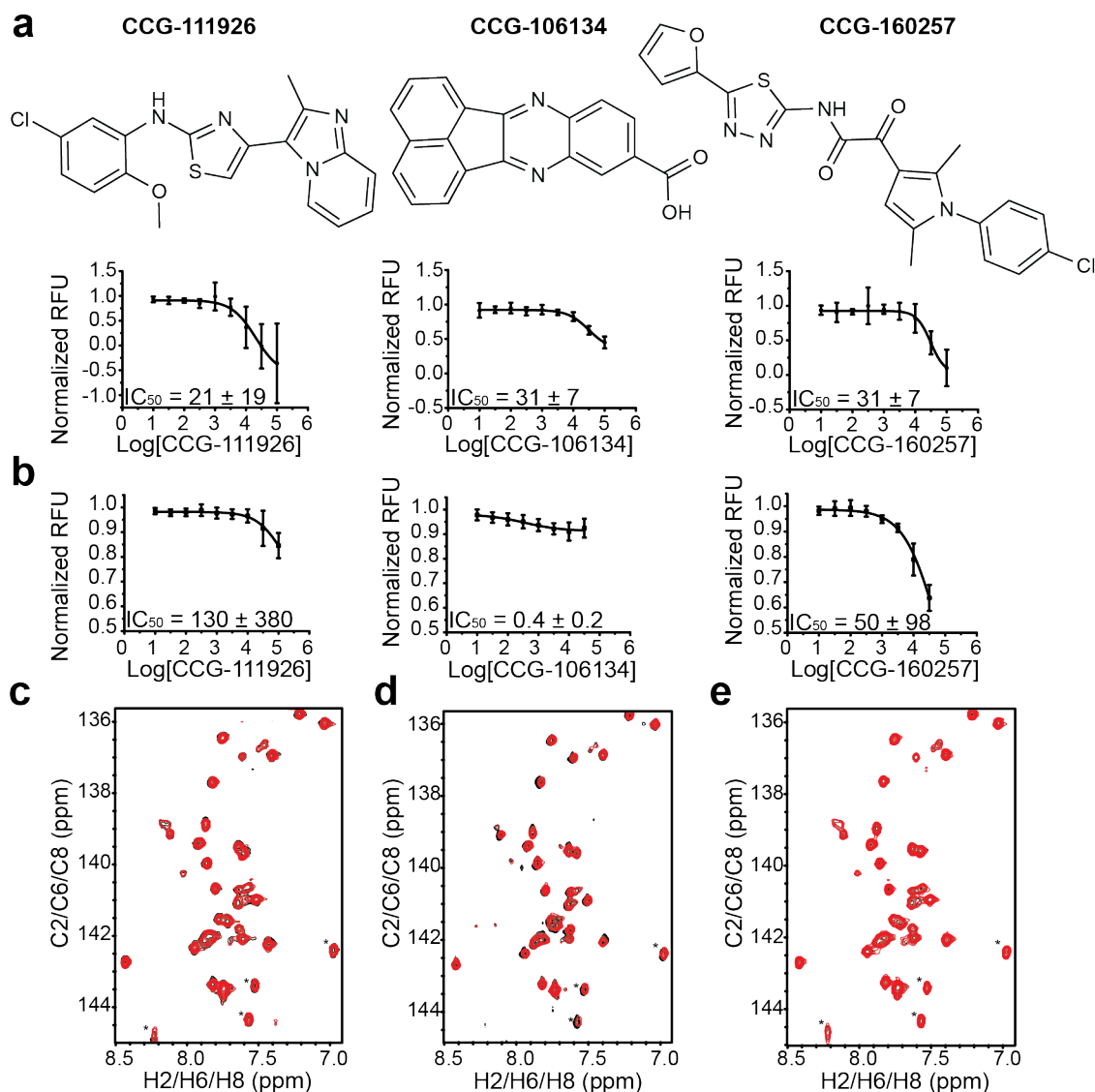
Supplemental Figures and Tables



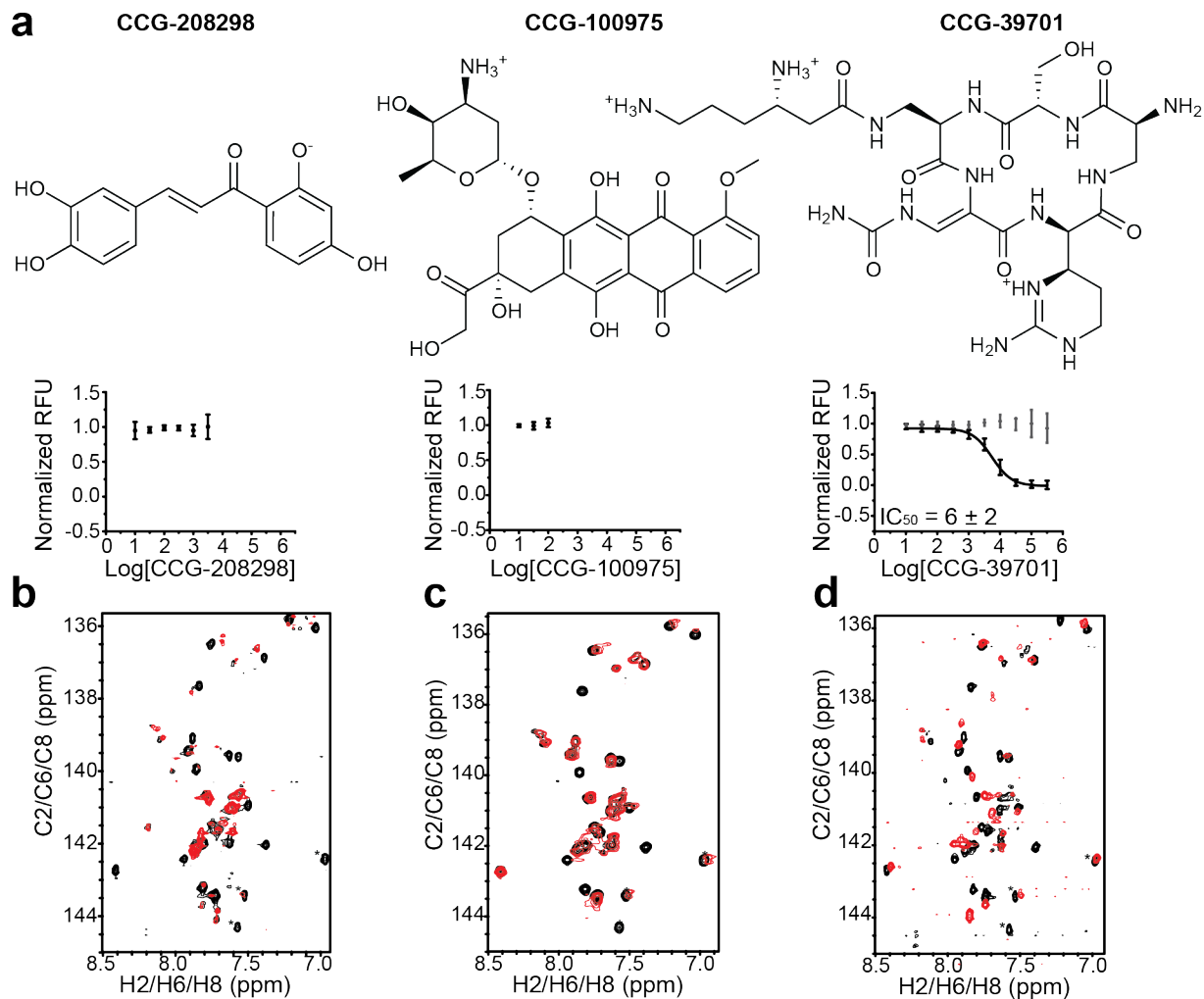
Supplementary Figure 1. HTS identified seven hit molecules that bind TAR and displace Tat peptide (see Methods). **a.** HTS workflow. **b.** Tat-displacement assays for the HTS hit molecules in the absence (black) and presence (gray) of 100-fold excess tRNA. **c-f.** Overlay of SOFAST- $[^1\text{H}-^{13}\text{C}]$ HMQC¹ NMR spectra of 50 μM TAR free (black) and in the presence of 3X hit molecule (red, purple or blue). Spectra are overlaid for hits that induced similar chemical shift perturbations: **c.** CCG-208662 (red) and CCG-208677 (blue); **d.** CCG-133879 (red), CCG-133868 (purple) and CCG-133895 (blue); **e.** CCG-133905 (red); and **f.** CCG-133994 (red). (*) designates folded peaks



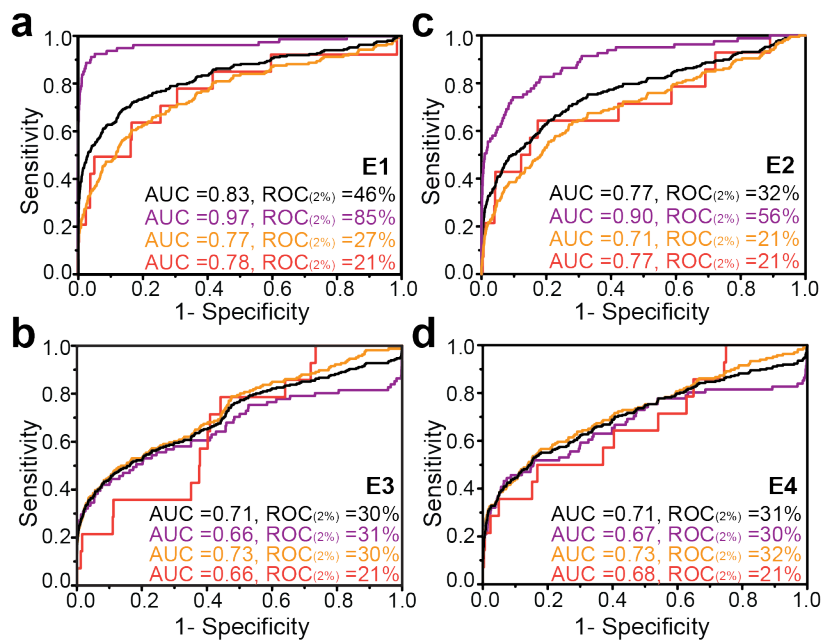
Supplementary Figure 2. Experiments to detect potential false negatives. Molecules with chemical similarity to hit molecules do not **a.** displace Tat peptide (points saturating the fluorescence reader are removed) or **b.** bind to TAR based on SOFAST- ^1H - ^{13}C HMQC¹ NMR chemical shift mapping employing 50 μM TAR. Shown are spectra with (red) and without (black) 3X small molecule. (*) designates folded peaks.



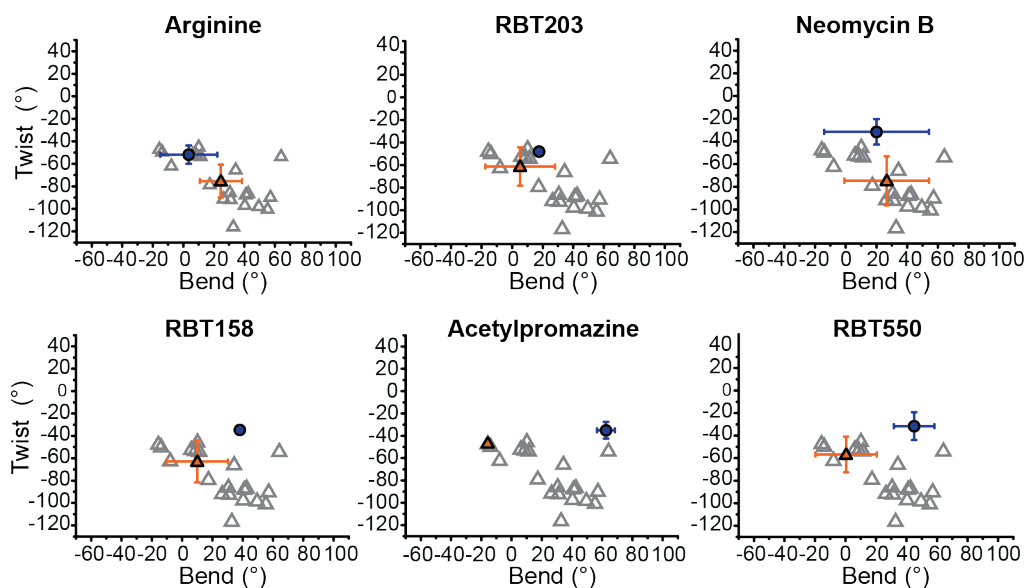
Supplementary Figure 3. Identifying false positive molecules from HTS using NMR. **a.** Tat-displacement assay showing activity for three molecules that were identified as hits by HTS, but that did not bind TAR by NMR. **b.** Tat-only control for the three molecules showing ambiguous activity. **c-e.** SOFAST- $[^1\text{H}-^{13}\text{C}]$ HMQC 1 NMR spectra of 50 μM TAR both free (black) and in the presence of **c.** 6X CCG-111926 (red), **d.** 4X CCG-106134 (red), and **e.** 3X CCG-160257 (red). (*) designates folded peaks.



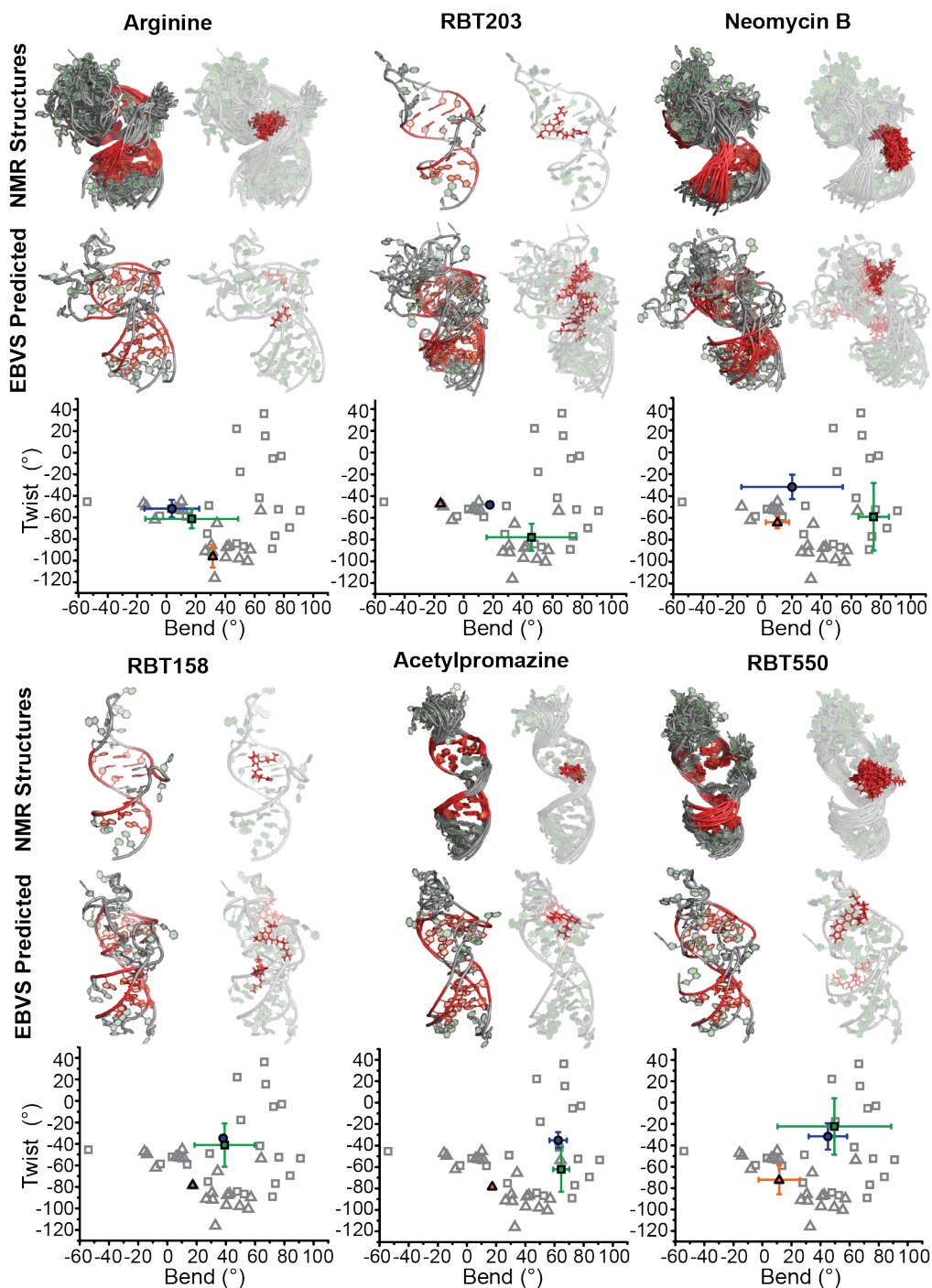
Supplementary Figure 4. False negative hits from HTS identified by testing a random set of nine molecules from within the top 3% of docking scores. **a.** Tat-displacement assays for CCG-208298 and CCG-100975, which have fluorescence interference with the assay at high concentrations (points saturating the fluorescence reader are removed); and CCG-39701, which was solubilized in water rather than DMSO. **b-d,** SOFAST- ^1H - ^{13}C HMQC 1 NMR spectra of 50 μM TAR both free (black) and in the presence of 3X molecule (red): **b.** 3X CCG-208298 **c.** 3X CCG-100925 and **d.** 3X CCG-39701. (*) designates folded peaks.



Supplementary Figure 5. ROC curves for EBVS against TAR ensembles **a.** E1, **b.** E2, **c.** E3 and **d.** E4 for all 247 hits (black), aminoglycoside hits (purple), non-aminoglycoside hits (orange) and cell-active hits (red).

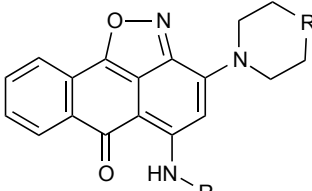
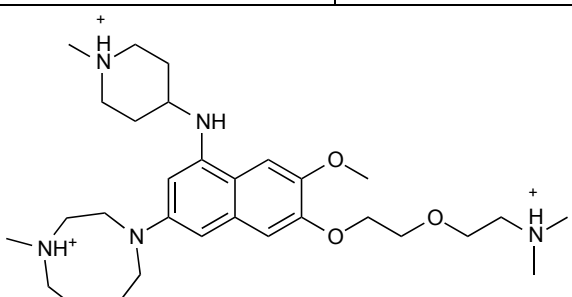
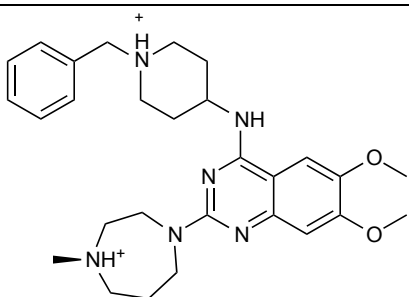


Supplementary figure 6. Inter-helical bend (β_h) and twist ($\alpha_h + \gamma_h$) angles² (negative and positive $\alpha_h + \gamma_h$ values correspond to over- and under-twisting respectively) averaged over all models in the NMR structure (blue circles) and the Boltzmann-weighted angles predicted by EBVS for the randomly selected ensemble, E3, averaged over 20 docking runs (orange triangle). Also shown are the angles for individual conformers in the E3 ensemble (open triangles).



Supplementary Figure 7. Analysis of docking predicted poses for six ligand-bound TAR complexes when using a docking thoroughness of twenty repeated five times. For each small molecule, NMR structures (all models) are compared to docking predicted structures (all conformations > 25% populated over five docking runs). Colored in red are the base pairs in the upper and lower stems used to superimpose the RNA structures (left) and the small molecule (right). Also shown are the inter-helical bend (β_h) and twist ($\alpha_h + \gamma_h$) angles² (negative and positive $\alpha_h + \gamma_h$ values correspond to

over- and under-twisting respectively) averaged over all models in the NMR structure (blue circles) and the Boltzmann-weighted angles predicted by EBVS averaged over 5 docking runs for the parent ensemble, E0, (green squares) and the random ensemble, E3, (orange triangles). Also shown are the angles for individual conformers in the parent ensemble, E0, (open squares) and random ensemble, E3, (open triangles).

Chemical Structure	Molecule Name	IC ₅₀ (μM)	100X tRNA IC ₅₀ (μM)	
	$R1 = \text{C}(=\text{O})\text{OCH}_2$ $R2 = \text{C}(\text{CH}_3)\text{CH}_2\text{NH}_2^+$	CCG-133994	12 ± 4	16 ± 5
	$R1 = \text{N}(\text{CH}_3)$ $R2 = \text{C}(\text{OH})\text{H}_2$	CCG-133895	17 ± 1	29 ± 17
	$R1 = \text{N}(\text{CH}_3)$ $R2 = \text{C}(\text{CH}_3)$	CCG-133868	31 ± 7	21 ± 10
	$R1 = \text{N}(\text{CH}_2\text{CH}_3)$ $R2 = \text{C}(\text{OH})\text{H}_2$	CCG-133905	53 ± 30	12 ± 1
	$R1 = \text{N}(\text{CH}_2\text{CH}_2\text{OH})$ $R2 = \text{C}(\text{CH}_3)$	CCG-133879	29 ± 8	24 ± 2
	CCG-208662	41 ± 14	NA	
	CCG-208677	55 ± 13	NA	

Supplementary Table 1. Hit Molecules identified by HTS with IC₅₀ values from the Tat-displacement assay in the presence and absence of 100-fold excess tRNA.

Supplementary Table 2. Table of known TAR binders taken from the literature.

(Provided as Excel Spreadsheet)

Molecule	Structure	N	CN	RDC RMSD (Hz)	R
Argininamide	NMR	29	1.85	5.98	0.87
	E0 Docking	29	2.12	5.35	0.86
	E3 Docking	29	1.90	5.66	0.82
Acetylpromazine	NMR	30	2.00	8.15	0.91
	E0 Docking	30	2.62	9.34	0.89
	E3 Docking	30	1.95	19.53	0.46

Supplementary Table 3. RAMAH³ analysis to determine the agreement between published ligand-bound TAR RDCs^{4,5} and the lowest energy bound-TAR structures from NMR^{6,7} and docking. Shown are the number of RDCs (N), condition number (CN), root mean-square deviation (RMSD), and correlation coefficient (R) between measured and back-predicted RDCs.

SUPPLEMENTARY REFERENCES

1. Sathyamoorthy, B., Lee, J., Kimsey, I., Ganser, L. R. & Al-Hashimi, H. Development and application of aromatic [¹³C, ¹H] SOFAST-HMQC NMR experiment for nucleic acids. *J. Biomol. NMR* **60**, 77–83 (2014).
2. Bailor, M. H., Mustoe, A. M., Brooks, C. L. & Al-Hashimi, H. M. 3D maps of RNA interhelical junctions. *Nat. Protoc.* **6**, 1536–1545 (2011).
3. Hansen, A. L. & Al-Hashimi, H. M. Insight into the CSA tensors of nucleobase carbons in RNA polynucleotides from solution measurements of residual CSA: towards new long-range orientational constraints. *J. Magn. Reson.* **179**, 299–307 (2006).
4. Zhang, Q., Stelzer, A. C., Fisher, C. K. & Al-Hashimi, H. M. Visualizing spatially correlated dynamics that directs RNA conformational transitions. *Nature* **450**, 1263–1267 (2007).
5. Pitt, S. W., Majumdar, A., Serganov, A., Patel, D. J. & Al-Hashimi, H. M. Argininamide binding arrests global motions in HIV-1 TAR RNA: comparison with Mg²⁺-induced conformational stabilization. *J. Mol. Biol.* **338**, 7–16 (2004).
6. Aboul-ela, F., Karn, J. & Varani, G. The structure of the human immunodeficiency virus type-1 TAR RNA reveals principles of RNA recognition by Tat protein. *J. Mol Biol.* **253**, 313–332 (1995).
7. Du, Z., Lind, K. E. & James, T. L. Structure of TAR RNA complexed with a Tat-TAR interaction nanomolar inhibitor that was identified by computational screening. *Chem. Biol.* **9**, 707–712 (2002).

SUPPLEMENTAL TABLE 2 REFERENCES

1. Cecchetti, V. *et al.* 6-Aminoquinolones as new potential anti-HIV agents. *J. Med. Chem.* **43**, 3799–3802 (2000).
2. Manfroni, G. *et al.* Synthesis and biological evaluation of 2-phenylquinolones targeted at Tat/TAR recognition. *Bioorganic Med. Chem. Lett.* **19**, 714–717 (2009).

3. Gatto, B. *et al.* 2-Phenylquinolones as inhibitors of the HIV-1 Tat-TAR interaction. *ChemMedChem* **4**, 935–938 (2009).
4. Litovchick, A., Evdokimov, A. G. & Lapidot, A. Arginine-aminoglycoside conjugates that bind to HIV transactivation responsive element RNA in vitro. *FEBS Lett.* **445**, 73–79 (1999).
5. Lapidot, A., Vijayabaskar, V., Litovchick, A., Yu, J. & James, T. L. Structure–activity relationships of aminoglycoside–arginine conjugates that bind HIV-1 RNAs as determined by fluorescence and NMR spectroscopy. *FEBS Lett.* **577**, 415–421 (2004).
6. Faber, C., Sticht, H., Schweimer, K. & Rösch, P. Structural rearrangements of HIV-1 Tat-responsive RNA upon binding of neomycin B. *J. Biol. Chem.* **275**, 20660–20666 (2000).
7. Hamasaki, K. & Ueno, A. Aminoglycoside antibiotics, neamine and its derivatives as potent inhibitors for the RNA-protein interactions derived from HIV-1 activators. *Bioorganic Med. Chem. Lett.* **11**, 591–594 (2001).
8. Blount, K. F., Zhao, F., Hermann, T. & Tor, Y. Conformational constraint as a means for understanding RNA-aminoglycoside specificity. *J. Am. Chem. Soc.* **127**, 9818–9829 (2005).
9. Blount, K. F. & Tor, Y. Using pyrene-labeled HIV-1 TAR to measure RNA-small molecule binding. *Nucleic Acids Res.* **31**, 5490–5500 (2003).
10. Riguet, E., Désiré, J., Bailly, C. & Décout, J. L. A route for preparing new neamine derivatives targeting HIV-1 TAR RNA. *Tetrahedron* **60**, 8053–8064 (2004).
11. Riguet, E. *et al.* Neamine dimers targeting the HIV-1 TAR RNA. *Bioorganic Med. Chem. Lett.* **15**, 4651–4655 (2005).
12. Xu, Y. *et al.* Synthesis and evaluation of novel neamine derivatives effectively targeting to RNA. *Bioorganic Med. Chem. Lett.* **19**, 2103–2106 (2009).
13. Ironmonger, A. *et al.* Scanning conformational space with a library of stereo- and regiochemically diverse aminoglycoside derivatives: the discovery of new ligands for RNA hairpin sequences. *Org. Biomol. Chem.* **5**, 1081–1086 (2007).

14. Kumar, S. *et al.* Click dimers to target HIV TAR RNA conformation. *Biochemistry* **51**, 2331–2347 (2012).
15. Ranjan, N. *et al.* Recognition of HIV-TAR RNA using neomycin-benzimidazole conjugates. *Bioorganic Med. Chem. Lett.* **23**, 5689–5693 (2013).
16. Raghunathan, D. *et al.* TAR-RNA recognition by a novel cyclic aminoglycoside analogue. *Nucleic Acids Res.* **34**, 3599–3608 (2006).
17. Yajima, S., Shionoya, H., Akagi, T. & Hamasaki, K. Neamine derivatives having a nucleobase with a lysine or an arginine as a linker, their synthesis and evaluation as potential inhibitors for HIV TAR-Tat. *Bioorganic Med. Chem.* **14**, 2799–2809 (2006).
18. Xu, Y., Jin, H., Yang, Z., Zhang, L. & Zhang, L. Synthesis and biological evaluation of novel neamine-nucleoside conjugates potentially targeting to RNAs. *Tetrahedron* **65**, 5228–5239 (2009).
19. Hwang, S. *et al.* Discovery of a small molecule Tat-trans-activation-responsive RNA antagonist that potently inhibits human immunodeficiency virus-1 replication. *J. Biol. Chem.* **278**, 39092–39103 (2003).
20. Mei, H. Y. *et al.* Inhibitors of protein-RNA complexation that target the RNA: specific recognition of human immunodeficiency virus type 1 TAR RNA by small organic molecules. *Biochemistry* **37**, 14204–14212 (1998).
21. Sztuba-Solinska, J. *et al.* Identification of biologically active, HIV TAR RNA-binding small molecules using small molecule microarrays. *J. Am. Chem. Soc.* **136**, 8402–8410 (2014).
22. He, M. *et al.* Synthesis and assay of isoquinoline derivatives as HIV-1 Tat-TAR interaction inhibitors. *Bioorganic Med. Chem. Lett.* **15**, 3978–3981 (2005).
23. Yu, F. *et al.* Design, synthesis, and biological evaluation of novel substituted [1,2,3]triazolo[4,5-d]pyrimidines as HIV-1 Tat-TAR interaction inhibitors. *Pure Appl. Chem.* **82**, 339–347 (2010).
24. Peytou, V. *et al.* Synthesis and antiviral activity of ethidium-arginine conjugates directed against the TAR RNA of HIV-1. *J. Med. Chem.* **42**, 4042–4053 (1999).

25. Schüller, A. *et al.* The concept of template-based de novo design from drug-derived molecular fragments and its application to TAR RNA. *J. Comput. Aided Mol. Des.* **22**, 59–68 (2008).
26. Davidson, A., Begley, D.W., Lau, C., & Varani, G. A small molecule probe induces a conformation in HIV TAR RNA capable of binding drug-like fragments. *J. Mol. Biol.* **410**, 984–996 (2012).
27. Gelus, N. *et al.* Inhibition of HIV-1 Tat-TAR interaction by diphenylfuran derivatives : effects of the terminal basic side chains. *Bioorg. Med. Chem.* **7**, 1089–1096 (1999).
28. Xiao, G. *et al.* Inhibition of the HIV-1 Rev-RRE complex formation by unfused aromatic cations. *Bioorg. Med. Chem.* **9**, 1097–1113 (2001).
29. Mischiati, C. *et al.* Aromatic polyamidines inhibiting the Tat-induced HIV-1 transcription recognize structured TAR-RNA. *Antisense Nucleic Acid Drug Dev* **11**, 209–217 (2001).
30. Mischiati, C. *et al.* Binding of hybrid molecules containing pyrrolo [2,1-c][1,4]benzodiazepine (PBD) and oligopyrrole carriers to the human immunodeficiency type 1 virus TAR-RNA. *Biochem. Pharmacol.* **67**, 401–410 (2004).
31. Zhao, P., Jin, H.-W., Yang, Z.-J., Zhang, L.-R. & Zhang, L.-H. Solid-phase synthesis and evaluation of TAR RNA targeted β -carboline–nucleoside conjugates. *Org. Biomol. Chem.* **6**, 3741–3750 (2008).
32. Duca, M., Malnuit, V., Barbault, F. & Benhida, R. Design of novel RNA ligands that bind stem-bulge HIV-1 TAR RNA. *Chem. Commun.* **46**, 6162–6164 (2010).
33. Blount, K. F. & Tor, Y. A tale of two targets: differential RNA selectivity of nucleobase-aminoglycoside conjugates. *ChemBioChem* **7**, 1612–1621 (2006).
34. Joly, J. P. *et al.* Artificial nucleobase-amino acid conjugates: a new class of TAR RNA binding agents. *Chem. Eur. J.* **20**, 2071–2079 (2014).
35. Murchie, A. I. H. *et al.* Structure-based drug design targeting an inactive RNA conformation: exploiting the flexibility of HIV-1 TAR RNA. *J. Mol. Biol.* **336**, 625–638 (2004).
36. Filikov, A. V. *et al.* Identification of ligands for RNA targets via structure-based virtual screening: HIV-1 TAR. *J. Comput. Aided Mol. Des.* **14**, 593–610 (2000).

37. Du, Z., Lind, K. E. & James, T. L. Structure of TAR RNA complexed with a Tat-TAR interaction nanomolar inhibitor that was identified by computational screening. *Chem. Biol.* **9**, 707–12 (2002).
38. Lind, K. E., Du, Z., Fujinaga, K., Peterlin, B. M. & James, T. L. Structure-based computational database screening, in vitro assay, and NMR assessment of compounds that target TAR RNA. *Chem. Biol.* **9**, 185–193 (2002).
39. Mayer, M. *et al.* Synthesis and testing of a focused phenothiazine library for binding to HIV-1 TAR RNA. *Chem. Biol.* **13**, 993–1000 (2006).
40. Renner, S. *et al.* New inhibitors of the Tat-TAR RNA interaction found with a ‘fuzzy’ pharmacophore model. *ChemBioChem* **6**, 1119–1125 (2005).
41. Stelzer, A. C. *et al.* Discovery of selective bioactive small molecules by targeting an RNA dynamic ensemble. *Nat. Chem. Biol.* **7**, 553–559 (2011).
42. Tao, J. & Frankel, A. D. Specific binding of arginine to TAR RNA. *Proc. Natl. Acad. Sci.* **89**, 2723–2726 (1992).
43. Bailly, C., Colson, P., Houssier, C. & Hamy, F. The binding mode of drugs to the TAR RNA of HIV-1 studied by electric linear dichroism. *Nucleic Acids Res.* **24**, 1460–1464 (1996).
44. Mei, H. Y. *et al.* Inhibition of an HIV-1 Tat-derived peptide binding to TAR RNA by aminoglycoside antibiotics. *Bioorganic Med. Chem. Lett.* **5**, 2755–2760 (1995).
45. Yu, X., Lin, W., Pang, R. & Yang, M. Design, synthesis and bioactivities of TAR RNA targeting β -carboline derivatives based on Tat-TAR interaction. *Eur. J. Med. Chem.* **40**, 831–839 (2005).
46. Hamy, F. *et al.* A new class of HIV-1 Tat antagonist acting through Tat-TAR inhibition. *Biochemistry* **37**, 5086–5095 (1998).
47. Tanrikulu, Y. *et al.* Scaffold hopping by ‘fuzzy’ pharmacophores and its application to RNA targets. *ChemBioChem* **8**, 1932–1936 (2007).